

1 **Large-scale secretome analyses unveil a superior immunosuppressive**
2 **phenotype from umbilical cord stromal cells compared to other adult**
3 **mesenchymal stromal cells**

4 A. Islam¹, I. Urbarova², J.A. Bruun² and I. Martinez-Zubiaurre^{1*}

5

6 1. Department of Clinical Medicine, University of Tromsø, Norway

7 2. Tromsø University Proteomics Platform, Department of Medical Biology, University of
8 Tromsø, Norway

9

10

11

12

13 Corresponding author:

14 Professor Inigo Martinez-Zubiaurre

15 Department of Clinical Medicine, University of Tromsø

16 9037 Tromsø, Norway

17 Email: inigo.martinez@uit.no

18 Phone: (0047)77644686

19

20

Abstract

21
22 Mesenchymal stromal cells (MSCs) with regenerative and immunomodulatory potential are
23 being investigated as a potential therapeutic tool for cartilage lesions. MSCs express a wide
24 variety of bioactive molecules including cytokines, trophic factors, and proteases, which act in
25 a paracrine fashion to modulate the tissue microenvironment. Yet, little is known about the
26 divergence of these signalling molecules between MSCs populations from adult or young
27 tissues. This makes it challenging to decide the optimal source of MSCs for a specific clinical
28 application. In this study, we investigated cell secretomes from cultured human stromal cells
29 harvested from Hoffa's fat pad (HFSPCs), synovial membrane (SMSCs), umbilical cord
30 (UCSCs) and cartilage (ACs) by quantitative LC-MS/MS proteomics. We also performed
31 multiplex protein arrays and functional assays to compare the constitutive immunomodulatory
32 capabilities of different MSCs. Proteins involved in extracellular matrix degradation and
33 inflammation such as MMPs, IL-17, and complement factors were significantly downregulated
34 in UCSCs compared to other cell types. Additionally, we found enhanced expression of TGF-
35 β 1 and PGE2 in UCSCs supernatants. UCSCs were superior in inhibiting peripheral blood
36 mononuclear cells proliferation, migration and TNF- α and IFN- γ secretion compared to ACs,
37 HFSPCs and SMSCs. Although all cell types could repress HLA-DR surface expression and
38 cytokine release by activated macrophages, only UCSCs significantly blocked IL-6 and IL-12
39 production. Our data demonstrate that stromal cells from umbilical cords display superior anti-
40 inflammatory and immunosuppressive properties than stromal cells from adult tissues. This
41 Allogeneic cell source could potentially be considered as an adjuvant therapy for articular
42 cartilage repair.

43

44

45

Introduction

46 Articular cartilage lesions associate with pain, discomfort, and inflammation in the synovial
47 joint, which subsequently restrict the function of articular activities. Mechanical trauma or
48 degenerative diseases are the major causes of articular cartilage injuries. Traumatic cartilage
49 lesions, on the other hand, increase the risk of developing osteoarthritis (OA) by more than four
50 times (Muthuri *et al.*, 2011). This fast-growing chronic disease is expected to be the fourth
51 leading cause of disability by the year 2020 (Cross *et al.*, 2014). Commonly used surgical and
52 nonsurgical OA treatment modalities include intra-articular injections of soluble materials such
53 as corticosteroids or hyaluronate, autologous blood products, nonsteroidal anti-inflammatory
54 drugs (NSAIDs), and arthroscopic lavage. These procedures improve OA symptoms to a certain
55 degree but do not heal completely the progressive loss of joint functions (Lee and Wang, 2017;
56 Wolfstadt *et al.*, 2015). Additionally, the treatment of localised cartilage injuries with cell-based
57 therapies benefit patients from debilitating knee functions and also prevents the onset of
58 developing secondary OA (Ogura *et al.*, 2017). Although autologous chondrocytes have been
59 used as an intuitive source for cell-based therapy, in recent years, mesenchymal stromal cells
60 (MSCs) are gaining attention as an alternative and potentially effective therapeutic tool for
61 cartilage lesions.

62 MSCs have been successfully isolated and expanded *in vitro* from numerous tissues sources.
63 Many scholars in the field support the notion that MSCs represent a defined population of
64 multipotent progenitor cells residing in the perivascular niche of nearly all human tissues,
65 although different views exist (Crisan *et al.*, 2008; Guimaraes-Camboa *et al.*, 2017). MSCs
66 differentiation capacity and immunomodulatory properties have been demonstrated *in vitro*
67 irrespective of tissue sources (Ghannam *et al.*, 2010). However, *in vitro* studies have shown
68 that MSCs from different origins differ in their lineage-specific differentiation capacity and
69 their functional potential (Garcia *et al.*, 2016; Islam *et al.*, 2016; Subramanian *et al.*, 2015). In

70 addition, a systematic review of intra-articular injection of bone marrow MSCs in humans
71 concluded that articular stem cells therapies are safe (Peeters *et al.*, 2013). Some preclinical
72 studies in animals have demonstrated the *in vivo* efficacy of MSCs from different sources in
73 OA management including autogenic, allogeneic and xenogeneic cell sources. However, none
74 of these studies has compared the optimal source of MSCs (Ozeki *et al.*, 2016; Saulnier *et al.*,
75 2015; Singh *et al.*, 2014; Yang *et al.*, 2015). Therefore, the choice of optimal source of MSCs
76 for a given clinical implication has yet to be elucidated.

77 Mechanistically, it is not well established how MSCs exert their effects *in vivo*. It was
78 previously believed that MSCs promote tissue regeneration by engraftment of cells in damaged
79 areas and transdifferentiating into tissue forming cells to promote repair (Liechty *et al.*, 2000).
80 Recently, the field has witnessed a paradigm shift in understanding the mechanism of action
81 elicited by MSCs, which highlights paracrine signalling and the release of potent bioactive
82 factors to modulate the microenvironment in benefit of tissue healing (Gnecchi *et al.*, 2016; Iso
83 *et al.*, 2007; Prockop, 2009). In the field of cartilage repair and OA, the fate of implanted cells
84 during biological repair procedures and their contribution to rebuilding the damaged tissue is
85 mostly unknown. Previous studies in animals suggest that most of the repaired tissue is
86 composed of cells of unknown origin migrating to the lesion (Dell'Accio *et al.*, 2003; Grande
87 *et al.*, 1989). A recent human clinical trial concluded that Allogeneic bone marrow MSCs
88 function as a source of stimulatory and trophic factors, which orchestrate tissue repair rather
89 than differentiating into the host tissue (de Windt *et al.*, 2017). However, clinical procedures
90 based on autologous MSCs transplantation, including bone marrow or adipose tissue MSCs,
91 may provide beneficial effects, but are associated with invasive harvesting procedures, two-
92 stage operations and long-time cell expansion *ex vivo*. Allogeneic MSCs harvested from
93 umbilical cords, amniotic membrane and placenta might represent alternative sources for one-
94 stage cell-based therapies. In addition to their pro-angiogenic properties, anti-inflammatory

95 phenotype, and multi-lineage differentiation potential, these Allogeneic MSCs are well
96 tolerated and elicit low immunogenic responses as their adult counterparts (Balasubramanian
97 *et al.*, 2012; Donders *et al.*, 2015). Unlike investigating neotissue forming ability, the role of
98 secreted bioactive molecules in the context of paracrine signalling and immunomodulation have
99 not been comprehensively explored between cells from adult joints and young cells. The aim
100 of this study was to find a suitable cell source that could serve as a potent immunomodulator to
101 mediate the tissue microenvironment.

102 In this study, we compared the secretome of culture-expanded cells harvested from four
103 different tissues sources comprising cartilage (ACs), Hoffa's fat pad (HFPCs), synovial
104 membrane (SMSCs) and umbilical cords (UCSCs). For analyses, mechanisms and pathways
105 relevant to cartilage and joint physiology including inflammation and immune regulation,
106 extracellular matrix (ECM) remodelling, mitotic factors and chondro-inductive molecules have
107 been considered. Proteins involved in ECM remodelling such as MMPs, complement factors,
108 and serpins were significantly downregulated in UCSCs compared to other cell types, whereas
109 cell signalling molecules such as TGF- β 1, MCP-1, and PDGFD were upregulated in UCSCs.
110 To evaluate the constitutive abilities of the different MSCs as immunomodulators, we compared
111 the immunoregulatory properties of supernatants from the different cell types by functional
112 immune assays. Our data revealed that UCSCs exhibit superior anti-inflammatory properties
113 and low catabolic phenotypes compared to ACs, HFPCs and SMSCs.

114

115 **Materials and Methods**

116 **Human Materials and Ethical statements**

117 Human samples were collected from the University Hospital of Northern Norway (UNN). The
118 Regional Ethical Committee (REK Nord 2014/920 and 2010/586) at the University of Tromsø

119 approved the study. Adult stromal cells were isolated from knee joint tissues of 25 patients aged
120 45 to 75 undergoing total knee replacement (TKR) to complete this study. A macroscopic
121 observation was made by the operating surgeon to assess the inflammatory states of the
122 samples. Patients with inflammatory joint diseases and very advanced OA were excluded;
123 however, both secondary posttraumatic and primary osteoarthritis patients were included in the
124 study. Fat pad and synovial membrane tissues were harvested from TKR patients. UCSCs were
125 isolated from seven umbilical cords immediately after birth. Buffy-coats for isolation of
126 peripheral blood mononuclear cells (PBMCs) were collected from healthy donors from the local
127 blood bank (REK Nord 2014/401). All patients provided written informed consent.

128 **Isolation and culture of human stromal cells**

129 Macroscopically good-looking cartilage without any traces of bone, collected from femoral
130 heads during total knee replacements was used to isolate human chondrocytes. All cell types
131 were isolated using a mixed enzymatic-explant method as previously described (Islam *et al.*,
132 2016; Islam *et al.*, 2017). Briefly, all tissue specimens were washed three times with sterile
133 Dulbecco's phosphate buffered saline (PBS; Cat. no. D8537; Sigma-Aldrich) and minced into
134 small pieces for enzymatic digestion in collagenase XI solution (Cat. no. C9407; ≥ 800 units/mg
135 solid, Sigma-Aldrich) at a final concentration of 1.25 mg/mL on a shaker at 37 °C. Cartilage
136 tissue specimens were digested for 3-4 h, and other adult tissue specimens were digested only
137 for 1-1.5 h. UCSCs were isolated from cord matrix (also known as a mixed cord) using 1 h of
138 digestion. Partially digested tissues were centrifuged for 10 min at 800 xg and resuspended in
139 high glucose Dulbecco's Modified Eagle Medium (DMEM; Cat. no. D5796; Sigma-Aldrich)
140 before plating on a T-75 culture flask (Cat. no. 156499; Thermo Scientific). The culture medium
141 was supplemented with L-ascorbic acid (62 mg/L) (Cat. no.103033E; BDH Laboratory),
142 penicillin and streptomycin (1 %) (P/S; Cat. no. P4333; Sigma-Aldrich) and 20 % foetal bovine
143 serum to promote cell attachment (FBS; Cat. no. S0115; Biochrom). All cells were incubated

144 in a humidified atmosphere containing 5 % CO₂ at 37 °C. After the initial 24 h, primary cultures
145 were expanded in 10 % FBS supplemented medium, and the medium was changed every 3-4 d
146 until the cultures became confluent.

147 **Preparation of conditioned medium**

148 All cells were used for experimentation at passage 3-4. Serum-rich conditioned medium was
149 used in functional assays with peripheral blood mononuclear cells (PBMCs) and macrophages,
150 whereas serum-free conditioned medium was used for protein-arrays and secretomics. Upon
151 reaching 70-80 % confluence, culture flasks were thoroughly washed with warmed PBS, and
152 the medium was replaced with fresh medium containing high glucose DMEM and 1 % P/S
153 (with or without 10 % FBS). Serum-free medium was additionally supplemented with insulin-
154 transferrin-selenium supplement (1:1000) (ITS; Cat. no. 354351; Corning). Both serum-free
155 and serum-rich conditioned medium (CM) were collected after 48 h, centrifuged at 4500 xg for
156 10 min, filtered using 0.22 µm porous membrane and used immediately for experimentation or
157 stored at – 70 °C for further analysis. The number of cells was counted for each culture
158 condition and used to normalise the measured expression of cytokines and growth factors in
159 CM. In functional assays with PBMCs and macrophages, the fresh culture medium was diluted
160 with serum-rich CM (1:1) from different stromal cells.

161 **Quantitative and qualitative LC-MS/MS analysis**

162 Serum-free CM (6 mL) from all cultures were collected from T-75 culture flasks and
163 concentrated in PBS to a final volume of 500-800 µL using 5000 Da MWCO vivaspin column
164 (Cat. no. Z614440-25EA; Sigma-Aldrich) at 4500 xg for 20 min. Protein concentration was
165 measured using DC Protein Assay Kit (Cat. no. 5000116; Bio-Rad). Protein samples (100
166 µg/tube) were reduced in 5 mM dithiothreitol (Cat. no. D9779; Sigma-Aldrich) for 30 min at
167 70 °C. Samples were alkylated by incubation with 375 mM iodoacetamide (Cat. no. 90034;

168 Thermo Scientific) at room temperature for 30 min in the dark. Protein samples were collected
169 as dry pellets after overnight precipitation in pre-chilled acetone (Cat. no. 270725; Sigma-
170 Aldrich) at -20 °C. Dry pellets containing 100 µg protein were resuspended in 100 µL of 2 M
171 Urea (Cat. no. U1250; Sigma-Aldrich) with 50 mM TEAB. Only 25 µg of protein per sample
172 was taken for further analysis. Samples were pre-digested for 6 h with 1:100 (w/w) LysC
173 endopeptidase (Cat. no. 125-05061; Wako Chemicals) with 1 mM final concentration of CaCl₂,
174 followed by further dilution with 50 mM TEAB in 1 M Urea and digestion overnight in 1:20
175 (w/w) trypsin (Cat. no. V511A; Promega). A volume of 5 µL trifluoroacetic acid (10 %) (Cat.
176 no. 28904; Thermo Scientific) was added to each tube and centrifuged at 13000rpm for 10 min.
177 OMIX C18 tips were used for sample clean-up and concentration. Samples containing 0.2 %
178 formic acid (FA; Cat. no. 28905; Thermo Scientific) were loaded to a Thermo Fisher Scientific
179 EASY-nLC1000 system and EASY-Spray column (C18, 2 µm, 100 Å, 50 µm, 50 cm). Peptides
180 were fractionated using a 2-100 % acetonitrile (Cat. no. 51101; Thermo Scientific) gradient in
181 0.1 % FA at a flow rate of 250 nL/min over 180 min. The separated peptides were analysed
182 using a Thermo Scientific Q-Exactive mass spectrometer. Data were collected by a Top10
183 method in data-dependent mode. The raw data were processed using MaxQuant (v 1.5.6.0) for
184 label-free protein quantification (LFQ). MS/MS data were searched against the UniProt human
185 database from November 2016 to yield protein identification (false discovery rate (FDR) =
186 0.01). Parameters used for the search: fixed modification, carbamidomethylation of cysteines;
187 variable modifications, oxidation of methionine and acetylation of protein N-terminal; ion mass
188 tolerance, 4.5 ppm; fragment mass tolerance, 20 ppm; charge states, 2+, 3+ and 4+; Maximum
189 missed cleavages, 2; enzyme specificity, trypsin; and minimum number of unique peptides, 2.
190 Perseus 1.5.6.0 software was used for statistical analysis of identified proteins. All contaminants
191 were filtered out before log₁₀-transformation of data for further analysis. The log₁₀-
192 transformed intensities were normalised by subtracting the median. Data were grouped as ACs,

193 HFPSCs, SMSCs and UCSCs and analysed using a *t*-test, with a minimum of three valid values
194 in each group. Volcano plots for each comparison were generated to identify differentially
195 expressed proteins using FDR < 0.01.

196 **Multiplex protein arrays**

197 A panel of 36 specific proteins including cytokines, chemokines, matrix metalloproteinases
198 (MMPs) and growth factors was measured in the serum-free CM of all four stromal cell types
199 by immune-based protein arrays. A human cytokine magnetic 25-plex kit (Cat. no. LHC0009M;
200 Thermo Scientific) was used to measure the concentration of 18 cytokines (1:4 dilution)
201 involved in inflammation including GM-CSF, IFN- α , IFN- γ , IL-1 β , IL-1RA, IL-2, IL-2R, IL-
202 4, IL-5, IL-6, IL-7, IL-8, IL-10, IL-12 (p40/p70), IL-13, IL-15, IL-17 and TNF- α and 7
203 chemokines (1:4 dilution) including Eotaxin, IP-10, MCP-1, MIG, MIP-1 α , MIP-1 β and
204 RANTES. Fluorokine MAP human MMP base kit (Cat. no. LMP000; R&D) was used to
205 measure the concentration of MMP-1, MMP-3, MMP-7, MMP-9 and MMP-13 (1:5 dilution).
206 Quantitative measurements (two replicates) were performed according to manufacturers'
207 guidelines using Luminex Bio-Plex 200 system (Bio-Rad, USA). In addition, quantification of
208 PGE2 (Cat. no. KGE004B) and five growth factors including TGF- β 1 (Cat. no. DY240-05),
209 BMP-2 (Cat. no. DY355-05), IGF-1 (Cat. no. DY291-05), PDGF-AB (Cat. no. DY222) and
210 bFGF (Cat. no. DY233-05) was performed by ELISA. All ELISA kits were purchased from
211 R&D Systems and performed according to manufacturer instructions. Measured protein
212 concentrations were normalised with cell number at specific culture conditions and expressed
213 as pg/mL/10⁶ cells.

214 **Isolation and culture of human PBMCs**

215 PBMCs were isolated from buffy-coats ($n = 5$) of whole blood using lymphoprep (Cat. no.
216 1114545; Alere Technologies) following manufacturer instructions. Briefly, peripheral blood

217 was diluted in sterile PBS (1:1) and slowly layered over a lymphoprep gradient in a 50 mL tube.
218 The tube was centrifuged without a break at 800 xg for 30 min at room temperature. PBMCs
219 were collected from the gradient-interface with a Pasteur pipette, followed by washing three
220 times for 10 min at 400 xg with PBSA containing PBS and 0.2 % bovine serum albumin (BSA;
221 Cat. no. 130-091-376; Miltenyi Biotec). PBMCs were cultured in growth medium containing
222 Rosewell Park Memorial Institute medium (RPMI-1640; Cat. no. R8758; Sigma-Aldrich), 1 %
223 P/S and 10 % FBS in a humidified atmosphere (5 % CO₂) at 37 °C.

224 **PBMCs activation assays**

225 PBMCs proliferation was assessed using the carboxyfluorescein succinimidyl ester (CFSE)
226 dilution assay (Cat. no. 10009853; Cayman). Cultured PBMCs were washed in pre-warmed
227 sterile PBS and centrifuged at 400 xg for 5 min before incubating cells with CFSE for 15 min
228 at 1:400 dilution. CFSE-stained PBMCs were cultured in RPMI, 1 % P/S and 10 % FBS in a
229 24-well plate at a density of 10⁶ cells/well. PBMCs were stimulated with the mitogen
230 phytohemagglutinin (10 µg/mL) (PHA; Cat. no. 1249738; Roche) for 5 d to induce
231 proliferation. Half of the medium was replaced with fresh medium after the second day. The
232 proliferation assay was performed on a BD FACSAria III flow cytometer, and the data were
233 analysed by FlowJo software (Tree Star Inc., USA). CM from stromal cells was added to the
234 culture of PHA activated PBMCs from 1 d at 1:1 ratio with fresh culture medium. CM from
235 last 3 d during proliferation of PBMCs was collected to measure cytokine profiles. CM derived
236 from PBMCS was centrifuged at 4500 xg for 5 min and filtered by 0.22 µm porous membrane
237 before analysing TNF-α (Cat. no. DY210-05; R&D) and IFN-γ (Cat. no. DY285-05; R&D)
238 contents using ELISA.

239 **PBMCs migration assay**

240 PBMCs migration assay was performed by a Boyden chamber assay. PBMCs were activated
241 with PHA (10 µg/mL) for 48 h before performing the assay. Recombinant stromal cell-derived
242 factor-1 (100 ng/mL) (SDF-1; Cat. no. 300-28A; PeproTech) was used as a chemoattractant.
243 PBMCs (10⁶ cells/100 µL) were added to the top chamber of Transwell culture inserts (6.5 mm
244 diameter, 8 µm pores, Cat. no. CLS3464; Sigma-Aldrich). Bottom chambers contained either
245 growth medium or serum-rich CM from different stromal cells. After 2 h, PBMCs that migrated
246 to the lower chamber were harvested and washed in PBSA by centrifugation at 400 xg for 4 min
247 followed by resuspending in 0.5 ml of PBSA. Lymphocytes population was gated using
248 forward, and side scatter and counted on a BD FACSAria III flow cytometer.

249 **Isolation and culture of monocyte-derived macrophages**

250 Monocytes were isolated from PBMCs using CD14⁺ magnetic-activated cell sorting (MACS)
251 (Cat. no. 130-050-201; Miltenyi Biotec) with minor modification from manufacturer
252 guidelines. Briefly, PBMCs were washed in MACs buffer containing autoMACS rinsing
253 solution (Cat. no. 130-091-222; Miltenyi Biotec) and BSA (20:1) for 10 min at 4 °C. PBMCs
254 were incubated with CD14⁺ microbeads at a concentration of 10 µL/10⁷ in 40 µL of MACs
255 buffer for 15 min at 4 °C. PBMCs were rinsed in MACs buffer and resuspended in appropriate
256 volume before passing through MS column. CD14⁺ monocytes were eluted from the column
257 and washed with ice-cold MACs buffer. The purity of eluted monocytes was checked by flow
258 cytometry using anti-CD14-FITC conjugated antibody (Cat. no. 130-098-063; Miltenyi Biotec)
259 and its isotype control mouse IgG2a-FITC (Cat. no. 130-098-877). Fully transformed
260 macrophages (M0-M) were achieved after six days incubation of CD14⁺ monocytes in a
261 macrophage growing medium containing RPMI-1640, 1 % P/S, 10 % FBS and 100 ng/mL
262 Macrophage Colony Stimulating Factor (M-CSF; Cat no. 300-25; Peprotech) in a humidified
263 atmosphere (5 % CO₂) at 37 °C. The medium was replaced with fresh medium after 3 d.

264 **Macrophage polarisation assays**

265 For induction of M1 phenotype (M1-M), M0-M were plated in a 6-well plate at density of 2.5
266 x 10⁶ cells/well and stimulated with lipopolysaccharides (100 ng/mL) (LPS; Cat. no. L6529-
267 1MG; Sigma-Aldrich) and IFN- γ (20 ng/mL) (Cat. no. 300-02; PeproTech) for 48 h. To
268 investigate the effects of cell secretomes on M1-M polarisation, macrophage culture medium
269 was diluted with serum-rich CM (1:1) from different stromal cells. Macrophages were
270 harvested after 48 h and washed in MACs buffer before analysing on BD FACSAria III flow
271 cytometer. FlowJo software was used for analysing surface markers expression.

272 M1-M polarization was characterised by surface marker expression of CD40 (Cat. no. 130-099-
273 385; Miltenyi Biotec), CD64 (Cat. no. 130-100-415; Miltenyi Biotec), CD80 (Cat. no. 130-110-
274 371; Miltenyi Biotec), CD86 (Cat. no. 560957; BD Biosciences) and HLA-DR (Cat. no.
275 560943; BD Biosciences). All antibodies were PE-conjugated and analysed with respective
276 isotype controls, including mouse IgG1 (Cat. no. 130-098-845; Miltenyi Biotec), REA control
277 (Cat. no. 130-104-612; Miltenyi Biotec) and mouse IgG2a (Cat. no. 555574; BD Biosciences).

278 For induction of M2 phenotype (M2-M), M0-M were stimulated with dexamethasone (4
279 μ g/mL) (Cat. no. PZN-3103491; Galenpharma) for 48 h and characterised by surface marker
280 expression of CD163-FITC (Cat. no. 130-099-969; Miltenyi Biotec) and its isotype control
281 mouse IgG1-FITC (Cat. no. 130-098-847). To further investigate the effects of CM from all
282 cell types on M1-M polarisation, macrophage-CM was collected after 48 h, centrifuged at 4500
283 xg for 5 min and filtered by 0.22 μ m porous membrane. The concentration of TNF- α , IL-6 (Cat.
284 no DY206-05) and IL-12 (Cat. no. DY1240-05) were measured by ELISA. All ELISA kits were
285 purchased from R&D Systems.

286 **Statistical analyses**

287 All statistical analyses were performed using IBM SPSS statistics version 24 (Chicago, USA).
288 Data were analysed using non-parametric Kruskal-Wallis test, and significance values were
289 adjusted by Bonferroni correction for multiple comparisons. The level of significance was set

290 at $p < 0.05$. Results were presented as density graphs, where each donor plotted as a dot in the
291 dataset.

292 **Results**

293 **Comparative protein profiles in supernatants of different stromal cells by LC-MS/MS** 294 **proteomics**

295 All cell types were characterised by MSCs surface markers and retained similar characteristics
296 as shown in our previous study (Islam *et al.*, 2016). The cell secretome established in serum-
297 free conditioned media from each cell type (four unrelated donors per cell type) was analysed
298 by LC-MS/MS proteomics. Only proteins identified in at least three donors of each cell type
299 were considered for further analyses. Results showed more proteins identified in the
300 supernatants of ACs (709) compared to HFPSCs (641), SMSCs (567) and UCSCs (653) (Fig.
301 1A). Comparative analysis of identified proteins revealed 472 proteins present in the
302 supernatants of all cell types. Only a minor fraction of proteins was exclusively found in
303 supernatants of specific cell types, including 50 differentially expressed by UCSCs, 44 by ACs,
304 22 by HFPSCs and two by SMSCs. Hierarchical clustering of identified proteins revealed two
305 major clusters, where one cluster comprised the four donors of UCSCs, and the second cluster
306 comprised all stromal cells from adult tissues (Fig. 1B). Furthermore, among the stromal cells
307 from adult tissues, the four ACs donors were clearly separated from HFPSCs and SMSCs
308 donors. Identified proteins were divided into six groups according to their functions using Gene
309 Ontology Biological Process (GOBP) terms (Fig. 2A). Qualitative comparison of proteins in
310 different pathways revealed no significant differences between cell sources. Proteins involved
311 in the catabolic process and ECM remodelling were abundant in the supernatants of all cell
312 types. In addition, all stromal cells released similar percentage of proteins involved in
313 immunoregulation (~ 20 %) and secretion (~ 13 %) (Fig. 2A).

314 Quantitative analyses of protein expression were performed using the LFQ approach (Fig. 2B).
315 Six volcano plots representing all possible comparisons show differentially expressed proteins
316 by plotting Log₁₀ of the fold change on the X-axis and -Log₁₀ of the *p*-value on the Y-axis for
317 each comparison (*e.g.* HFPSCs vs ACs). Results revealed largest differences in protein
318 expression between UCSCs and adult stromal cells (*p* < 0.01). Proteins involved in cell
319 signalling such as TGF-β1, PDGFD, and MCP-1 were significantly upregulated in UCSCs,
320 while catabolic proteins such as MMPs, serpins, and complement factors were downregulated
321 compared to stromal cells from the adult origin (Fig. 2B). Notably, minor differences
322 particularly in ECM remodelling proteins such as MMPs, and serpins were observed while
323 comparing stromal cells from cartilage and synovium (Fig. 2B). Protein profiles belonging to
324 specific pathways (ECM remodelling, cell communication, and inflammation) were compared
325 among the four cell types (Fig. 3). Several MMPs, serpins, some complement factors, and heat
326 shock proteins were less expressed in UCSCs. On the other hand, some cell signalling
327 molecules including MCP-1, ITG-β1, PDGFD, CSF-1, HLA-C and TGF-β1 were more
328 abundant in the supernatants of UCSCs.

329 **Determination of cytokines and growth factors in supernatants by multiplex protein** 330 **arrays**

331 A panel of 18 selected cytokines involved in inflammation and immunoregulation was
332 measured in supernatants of all stromal cells. Only IL-4, IL-6, IL-8, IL-12 and IL-17 were
333 detected in supernatants of all cell types, whereas GM-CSF, IFN-α, IFN-γ, IL-1β, IL-1RA, IL-
334 2, IL-2R, IL-5, IL-7, IL-13, IL-15 and TNF-α could not be detected in any of the supernatants.
335 From the panel of chemokines, MCP-1, MIP-1α and RANTES were detected in all
336 supernatants, but Eotaxin, IP-10, MIG and MIP-1β could not be detected. Overall, the levels of
337 IL-6, MPC-1 and PGE₂ were increased in UCSCs supernatants compared to other cell types,
338 whereas the levels of IL-17, MIP-1α and RANTESs were decreased (Fig. 4). The concentration

339 of IL-17 and MIP-1 α was significantly lower in the supernatants of UCSCs compared to ACs,
340 and the levels of PGE2 was significantly higher in UCSCs supernatants compared to HFPSCs
341 (Fig. 4). Regarding expression of proteases, only MMP-13 was not detectable, whereas MMP-
342 1, MMP-3, MMP-7 and MMP-9 were detected to some degree in all serum-free CM (Fig. 5).
343 The secretion of MMP-1, MMP-3, MMP-7 and MMP-9 was in general lower in UCSCs cultures
344 compared to all other cell types. Significant differences were found for MMP-3 and MMP-7
345 when comparing UCSCs and ACs. The anabolic growth factors TGF- β 1, BMP-2 and bFGF
346 were detected at low levels in supernatants of the four cell sources, whereas IGF-1 and PDGF-
347 AB could not be detected. Importantly, TGF- β 1 was significantly elevated by UCSCs compared
348 to HFPSCs (Fig. 5).

349 **UCSCs supernatants exert stronger immunosuppressive effects on mitogen-activated** 350 **PBMCs**

351 To investigate the immunomodulatory effects of cell supernatants on activated PBMCs, we
352 performed *in vitro* proliferation and migration assays (Fig. 6A). Mitogen (phytohaemagglutinin,
353 PHA)-activated PBMCs were incubated for 5 d in the presence or absence of serum-containing
354 CM from the different cell types. Proliferation assays revealed that UCSCs supernatants
355 blocked PBMCs proliferation ($p = 0.06$) when compared with PHA-treated controls (Fig. 6A
356 and B). CM from ACs did not block PBMCs proliferation, while HFPSCs (71 ± 5 %) and
357 SMSCs (68 ± 3 %) had a minor effect. In migration assays, both UCSCs and SMSCs blocked
358 the migration of activated PBMCs compared to positive controls (38 ± 2.5 % and 38 ± 1.2 %
359 vs 44.2 ± 0.5 %, respectively) (Fig. 6B). To further investigate the immunomodulatory effects
360 of MSCs supernatants, we measured the expression of TNF- α and IFN- γ in PBMCs-CM. Values
361 were normalised against residual expression levels present in supernatants of stromal cells.
362 Supernatants from HFPSCs and SMSCs stimulated the production of TNF- α and IFN- γ above
363 the levels achieved by PHA treatments. Importantly, supernatants from UCSCs suppressed the

364 production of both TNF- α and IFN- γ by activated PBMCs, reaching significant differences
365 when compared to HFPSCs (Fig. 6C).

366 **UCSCs supernatants exert superior anti-inflammatory effects on M1 activated**
367 **macrophages**

368 Macrophage polarisation assay was performed as previously reported (Ambarus *et al.*, 2012;
369 Vogel *et al.*, 2014). A panel of costimulatory molecules and cytokines to characterise
370 macrophage polarisation was chosen based on validation tests using different stimulants. We
371 observed divergent expression of these markers in the presence of different stimulants. In
372 addition, we found IL-10 production as an irrelevant marker for M2 polarised macrophages. In
373 the validation study, we observed increased IL-10 production in the presence of LPS and IFN-
374 γ compared to dexamethasone or TGF- β and IL-4 stimulation. These discrepancies have also
375 been reported in other studies (Chanteux *et al.*, 2007; Vogel *et al.*, 2014). Moreover, we also
376 observed CD163 as a suitable marker for dexamethasone-stimulated M2 polarised
377 macrophages. The discrepancy concerning the expression of CD206 has also been demonstrated
378 in a previous study (Jaguin *et al.*, 2013).

379 In this study, immunomodulatory effects on M1 polarised macrophages were investigated by
380 characterisation of surface markers expression of CD40, HLA-DR, CD64, CD80, CD86 and
381 inflammatory cytokines release (Fig. 7). Supernatants from all stromal cell types suppressed
382 the surface expression of HLA-DR on activated macrophages, whereas only UCSCs
383 supernatants were able to significantly suppress the expression of CD40. On the other hand,
384 supernatants from ACs were able to increase the expression of the co-regulatory receptors
385 CD80 and CD86 above the levels of M1 activation (Fig. 7B). In contrast to ACs and UCSCs,
386 supernatants from HFPSCs and SMSCs increased the surface expression of CD64 above M1
387 activation levels. None of the supernatants was able to alter the expression of the M2 phenotype
388 marker CD163. Regarding cytokines profiles, CM from all cell types was able to reduce the

389 production of TNF- α , IL-6 and IL-12 by M1-M. Of note, a significant reduction of IL-6 and IL-
390 12 concentration was only achieved by UCSCs (Fig. 7C).

391 **Discussion**

392 The main objective of this study was to ascertain which source of stromal cells possesses the
393 most favourable phenotype for the treatment of hyaline cartilage lesions or chronic
394 inflammatory joint disorders. Given the importance of paracrine signalling of MSCs, we
395 performed large-scale comparative analyses of cell secretomes and conducted functional
396 studies with cell supernatants on immune cells to compare the constitutive immunomodulatory
397 capabilities of different MSCs. Overall, our results demonstrate that stromal cells from
398 umbilical cord matrix exhibit better anti-inflammatory and trophic effects when compared with
399 ACs, HFPSCs and SMSCs.

400 In our study, all cell sources have been expanded in monolayer cultures in the serum-
401 supplemented medium for some weeks, as done in standard cell transplantation procedures. To
402 facilitate the analyses of secretory profiles by LC-MS/MS proteomics, the media were
403 conditioned under serum-free conditions. Multiplex protein assays were performed with the
404 same serum-free CM that was used for proteomics, which allowed us to make direct
405 comparisons of results. However, functional assays with immune cells were done with serum-
406 supplemented CM, as serum deprivation has been shown to affect proliferation and induce
407 apoptosis in lymphocytes and macrophages, respectively (Sato *et al.*, 2009; Wei *et al.*, 2006).
408 Short periods of serum deprivation have been shown to not affect the cell viability of
409 mesenchymal cells (Boraldi *et al.*, 2008). However, some changes in the secretome could occur
410 upon changes in serum supplementation. We have analysed in parallel the expression of TNF-
411 α , IFN- γ , IL-6 and IL-12 in both serum-containing and serum-free CM from all four cell types
412 and only the expression of IL-6 was considerably changed in the presence of serum (Fig. 8).
413 Although we expect only minor phenotypic changes in cells associated with serum presence,

414 alterations in the expression of some bioactive molecules could occur and should be taken into
415 consideration.

416 Currently, MSCs are viewed as “drugstores” with the potential to modulate the phenotype,
417 migration and activation of resident tissue and inflammatory cells (Caplan and Correa, 2011).
418 These have lead researchers to study MSC-mediated paracrine effects and profiles of secreted
419 proteins from different mesenchymal stromal cell types. Previous studies comparing secretory
420 profiles from different MSCs sources highlight the existence of differentially expressed factors
421 with impact on angiogenesis, matrix remodelling, inflammation and immunosuppression
422 (Amable *et al.*, 2014; Dabrowski *et al.*, 2017; Hsiao *et al.*, 2012; Li *et al.*, 2015). Our qualitative
423 analyses using large-scale proteomic approach reveal similar protein profiles, where the
424 majority of identified proteins are present in all cell supernatants. However, after hierarchical
425 clustering of protein profiles from all donors, UCSCs secretomes single out from the other adult
426 cell sources (Fig. 1B). Quantitative analyses of the secretome data reveal that proteins involved
427 in cell signalling such as TGF- β 1 and PDGFD were significantly upregulated in UCSCs
428 supernatants, while catabolic proteins such as MMPs, serpins, and complement factors were
429 downregulated compared to stromal cells from the adult origin. TGF- β 1 is a master driver of
430 chondrogenesis and has been shown to ameliorate OA pathogenesis (Tang *et al.*, 2015; Zhang
431 *et al.*, 2015). In addition, TGF- β 1 has been shown to possess anti-apoptotic effects (Rehman *et*
432 *al.*, 2004). Observations from other studies are disparate and include cell sources that we have
433 not used; however, the superior anabolic phenotype of UCSCs, including highest expression of
434 TGF- β among the compared cell types, has also been observed recently by others (Dabrowski
435 *et al.*, 2017). Data from our multiplex protein analyses also confirmed the findings of LC-
436 MS/MS. It revealed a significant reduction of MMPs and increased expression of TGF- β 1 by
437 UCSCs, thus reasserting observations made in the large-scale proteomic approach. Altogether,

438 these observations highlight less catabolic phenotype of UCSCs compared to the three other
439 adult MSCs in the context of cartilage repair.

440 The immunomodulatory profile of the different MSCs was also investigated by proteomics and
441 multiplex arrays. Secretome analyses revealed comparable expression of complement
442 components, heat shock proteins, galectins and immunoregulators such as CSF-1, MCP-1, MIF
443 and TGF- β 1 among the different cell sources. In addition, our data from multiplex protein
444 arrays showed enhanced expression of the immunomodulators IL-6, MCP-1 and PGE2, and
445 reduced expression of IL-17 and MIP-1 α by UCSCs. IL-6 has an omnidirectional role in
446 maintaining biological functions. It has been reported to have deleterious effects in the joint
447 (Poree *et al.*, 2008; Sui *et al.*, 2009). However, selective depletion of IL-6 in animals is
448 associated with accelerated joint degeneration upon ageing (de Hooge *et al.*, 2005). Other
449 authors have demonstrated IL-6-dependent inhibition of local inflammation in experimental
450 arthritis (Bouffi *et al.*, 2010).

451 MCP-1 (also called CCL2), MIP-1 α (CCL3) and IL-17 are all potent inflammatory factors
452 mediating recruitment and activation of myeloid cells. Their presence is associated with
453 cartilage degeneration and progression of OA (Appleton *et al.*, 2015; Snelling *et al.*, 2017;
454 Wang *et al.*, 2017; Xu *et al.*, 2015; Zhao *et al.*, 2015). Mechanistically, IL-17 has been reported
455 to inhibit chondrogenesis and promote MMPs in chondrocytes (Benderdour *et al.*, 2002; Kondo
456 *et al.*, 2013). PGE2 is known to regulate the phenotype and functions of pro-inflammatory
457 macrophages and NK cells (Manferdini *et al.*, 2017), however, the overall role of this factor in
458 OA progression and cartilage homeostasis is still controversial (Bouffi *et al.*, 2010; Miwa *et al.*,
459 2000; Otsuka *et al.*, 2009). Despite the difficulty to reach general conclusions due to the
460 pleiotropic nature of many chemokines and cytokines, our observations based on the global
461 expression of released factors indicate that UCSCs display a more immunosuppressive and anti-
462 inflammatory phenotype than their adult counterparts.

463 To investigate further the paracrine potential of the different MSCs on immunomodulation we
464 conducted functional assays on lymphocytes and macrophages. Results follow the same trend
465 as the analyses made on protein profiles, highlighting the superior immunosuppressive
466 phenotype of UCSCs compared to the other MSCs. The ability of MSCs to regulate
467 inflammation and immunity has been the focus of intense research during recent years (Donders
468 *et al.*, 2018; von Bahr *et al.*, 2012). Many *in vitro* studies have shown that mesenchymal cells
469 from multiple sources, including differentiated connective tissue cells such as chondrocytes and
470 fibroblasts, have the potential to regulate inflammation and T-cell functions to some extent
471 (Bouffi *et al.*, 2011; Lohan *et al.*, 2016). Still, there is no consensus on which cell source is the
472 most powerful in this respect.

473 Most published studies have compared bone marrow, adipose tissue and foetal tissues with
474 different outcomes. Some comparative studies demonstrated bone marrow MSCs have slightly
475 superior immunosuppressive capacity than other MSCs (Heo *et al.*, 2016; Karaoz *et al.*, 2017).
476 In line with our observations, some groups have previously observed superior
477 immunosuppressive abilities by MSCs from cords (Jin *et al.*, 2013; Najar *et al.*, 2012). It is
478 important to mention that in our study MSCs were not primed with pro-inflammatory cytokines
479 during medium conditioning. Such experimental condition allowed us to investigate the
480 constitutive abilities of these cells without external stimuli. Priming of MSCs is extensively
481 documented in the published literature and has been recommended as a mandatory step to
482 unleash the full immunosuppressive potential of MSCs (Gomez-Aristizabal *et al.*, 2017; Najar
483 *et al.*, 2012; van Buul *et al.*, 2012). In agreement with our study, constitutive immunoregulation
484 by unstimulated MSCs has been previously observed (Saulnier *et al.*, 2015). In this context, *ex*
485 *vivo* priming of MSCs has been related with few controversial outcomes *in vivo* describing
486 increased immunogenicity of pre-stimulated MSCs (Papadopoulou *et al.*, 2012; Treacy *et al.*,
487 2014).

488 In clinical settings, MSCs from different sources have been investigated for the treatment of
489 focal cartilage lesions and OA (Lee and Wang, 2017). Articular chondrocytes, bone marrow
490 and adipose tissue stromal cells are the most commonly used sources for cartilage repair (Vonk
491 *et al.*, 2015). These studies mostly assessed safety and efficacy of used MSCs for specific
492 clinical implications. However, a comparative study in humans argued that autologous SMSCs
493 exert superior healing outcomes (Akgun *et al.*, 2015). On the other hand, in preclinical models,
494 MSCs from cords have been shown to exert immunosuppression and disease regression in
495 experimental models of OA and autoimmune disorders (Donders *et al.*, 2015; Saulnier *et al.*,
496 2015; Yang *et al.*, 2015). In contrast to MSCs from autologous sources, there are few ongoing
497 trials exploring the potential of allogeneic UCSCs for both OA management and focal cartilage
498 repair in humans (NCT02580695, NCT02291926, NCT03166865 and NCT03358654), without
499 published outcomes hitherto. Confirming the results of this comparative study in suitable
500 animal models would provide more insight into the use of UCSCs in the clinics.

501 **Conclusions**

502 Traditionally, the regenerative potential of MSCs has been directly linked to their multipotent
503 differentiation and tissue-forming capabilities. Nowadays, increasing attention is given to their
504 role as cellular modulators. In the field of articular cartilage lesions and degenerative joint
505 diseases, there is no consensus on the best cell source for treatment. Considering the relevance
506 of paracrine signalling, in this study we have compared the secretomes among MSCs from
507 different sources. Both the molecular analyses and the functional assays indicate that UCSCs
508 display superior anti-inflammatory and trophic effects compared to other MSCs from adult
509 tissues. The hypoimmunogenic nature of UCSCs, along with their high abundance, simple
510 isolation and favourable protein profiles makes this cell source an attractive tool for off-the-self
511 allogeneic adjuvant therapy.

512

Acknowledgements

513 The authors sincerely thank Drs. Geir Tore Abrahamsen and Gunnar Knutsen, University
514 Hospital of Northern Norway (UNN), for providing cartilage and Hoffa's fat pad biopsies,
515 Kirsten Synnøve Nilsen for her assistance in ELISA assays, Trine Kalstad for her support
516 during Luminex, Dr. Ruomei Li for providing reagents for LC-MS/MS, Dr. Rodrigo Berzaghi
517 and Kirsti Rønne for their endless support during experiments.

518

Availability of data and materials

519 The datasets used in this study are available from the corresponding author upon request.

520

Funding

521 This work had financial support from the University of Tromsø.

522

Authors' Contributions

523 AI primarily conducted the laboratory work, planned the study and prepared the manuscript.
524 IMZ participated in the conception of the study, data evaluation, edited and approved the final
525 draft of the manuscript. IU and JAB performed LC-MS/MS. All authors contributed to the data
526 interpretation of results, provided direction and comments on the manuscript.

527

Ethical statement

528 The Regional Ethical Committee of Northern Norway has approved the study (REK Nord
529 2014/920 and 2010/586).

530

Consent for publication

531 Not applicable

532

Competing interests

533 The authors declare no competing interests.

534

References

535 Akgun I, Unlu MC, Erdal OA, Ogut T, Erturk M, Ovali E, Kantarci F, Caliskan G,
536 Akgun Y (2015) Matrix-induced autologous mesenchymal stem cell implantation versus
537 matrix-induced autologous chondrocyte implantation in the treatment of chondral defects of the
538 knee: a 2-year randomized study. *Arch Orthop Trauma Surg* **135**: 251-263.

539 Amable PR, Teixeira MVT, Carias RBV, Granjeiro JM, Borojevic R (2014) Protein
540 synthesis and secretion in human mesenchymal cells derived from bone marrow, adipose tissue
541 and Wharton's jelly. *Stem Cell Research & Therapy* **5**: 53-53.

542 Ambarus CA, Krausz S, van Eijk M, Hamann J, Radstake TR, Reedquist KA, Tak PP,
543 Baeten DL (2012) Systematic validation of specific phenotypic markers for in vitro polarized
544 human macrophages. *J Immunol Methods* **375**: 196-206.

545 Appleton CT, Usmani SE, Pest MA, Pitelka V, Mort JS, Beier F (2015) Reduction in
546 disease progression by inhibition of transforming growth factor alpha-CCL2 signaling in
547 experimental posttraumatic osteoarthritis. *Arthritis Rheumatol* **67**: 2691-2701.

548 Balasubramanian S, Venugopal P, Sundarraj S, Zakaria Z, Majumdar AS, Ta M (2012)
549 Comparison of chemokine and receptor gene expression between Wharton's jelly and bone
550 marrow-derived mesenchymal stromal cells. *Cytotherapy* **14**: 26-33.

551 Benderdour M, Tardif G, Pelletier JP, Di Battista JA, Reboul P, Ranger P, Martel-
552 Pelletier J (2002) Interleukin 17 (IL-17) induces collagenase-3 production in human
553 osteoarthritic chondrocytes via AP-1 dependent activation: differential activation of AP-1
554 members by IL-17 and IL-1beta. *J Rheumatol* **29**: 1262-1272.

555 Boraldi F, Annovi G, Paolinelli-Devincenzi C, Tiozzo R, Quaglino D (2008) The effect
556 of serum withdrawal on the protein profile of quiescent human dermal fibroblasts in primary
557 cell culture. *Proteomics* **8**: 66-82.

558 Bouffi C, Bony C, Courties G, Jorgensen C, Noel D (2010) IL-6-dependent PGE2
559 secretion by mesenchymal stem cells inhibits local inflammation in experimental arthritis.
560 PLoS One **5**: e14247.

561 Bouffi C, Bony C, Jorgensen C, Noel D (2011) Skin fibroblasts are potent suppressors
562 of inflammation in experimental arthritis. Ann Rheum Dis **70**: 1671-1676.

563 Caplan AI, Correa D (2011) The MSC: an injury drugstore. Cell Stem Cell **9**: 11-15.

564 Chanteux H, Guisset AC, Pilette C, Sibille Y (2007) LPS induces IL-10 production by
565 human alveolar macrophages via MAPKinases- and Sp1-dependent mechanisms. Respir Res **8**:
566 71.

567 Crisan M, Yap S, Casteilla L, Chen CW, Corselli M, Park TS, Andriolo G, Sun B, Zheng
568 B, Zhang L, Norotte C, Teng PN, Traas J, Schugar R, Deasy BM, Badylak S, Buhring HJ,
569 Giacobino JP, Lazzari L, Huard J, Peault B (2008) A perivascular origin for mesenchymal stem
570 cells in multiple human organs. Cell Stem Cell **3**: 301-313.

571 Cross M, Smith E, Hoy D, Nolte S, Ackerman I, Fransen M, Bridgett L, Williams S,
572 Guillemin F, Hill CL, Laslett LL, Jones G, Cicuttini F, Osborne R, Vos T, Buchbinder R, Woolf
573 A, March L (2014) The global burden of hip and knee osteoarthritis: estimates from the global
574 burden of disease 2010 study. Ann Rheum Dis **73**: 1323-1330.

575 Dabrowski FA, Burdzinska A, Kulesza A, Sladowska A, Zolocinska A, Gala K, Paczek
576 L, Wielgos M (2017) Comparison of the paracrine activity of mesenchymal stem cells derived
577 from human umbilical cord, amniotic membrane and adipose tissue. J Obstet Gynaecol Res **43**:
578 1758-1768.

579 de Hooge AS, van de Loo FA, Bennink MB, Arntz OJ, de Hooge P, van den Berg WB
580 (2005) Male IL-6 gene knock out mice developed more advanced osteoarthritis upon aging.
581 Osteoarthritis Cartilage **13**: 66-73.

582 de Windt TS, Vonk LA, Slaper-Cortenbach ICM, Nizak R, van Rijen MHP, Saris DBF
583 (2017) Allogeneic MSCs and Recycled Autologous Chondrons Mixed in a One-Stage Cartilage
584 Cell Transplantation: A First-in-Man Trial in 35 Patients. *Stem Cells* **35**: 1984-1993.

585 Dell'Accio F, Vanlauwe J, Bellemans J, Neys J, De Bari C, Luyten FP (2003) Expanded
586 phenotypically stable chondrocytes persist in the repair tissue and contribute to cartilage matrix
587 formation and structural integration in a goat model of autologous chondrocyte implantation. *J*
588 *Orthop Res* **21**: 123-131.

589 Donders R, Bogie JFJ, Ravanidis S, Gervois P, Vanheusden M, Maree R,
590 Schrynemackers M, Smeets HJM, Pinxteren J, Gijbels K, Walbers S, Mays RW, Deans R, Van
591 Den Bosch L, Stinissen P, Lambrechts I, Gyselaers W, Hellings N (2018) Human Wharton's
592 Jelly-Derived Stem Cells Display a Distinct Immunomodulatory and Proregenerative
593 Transcriptional Signature Compared to Bone Marrow-Derived Stem Cells. *Stem Cells Dev* **27**:
594 65-84.

595 Donders R, Vanheusden M, Bogie JF, Ravanidis S, Thewissen K, Stinissen P, Gyselaers
596 W, Hendriks JJ, Hellings N (2015) Human Wharton's Jelly-Derived Stem Cells Display
597 Immunomodulatory Properties and Transiently Improve Rat Experimental Autoimmune
598 Encephalomyelitis. *Cell Transplant* **24**: 2077-2098.

599 Garcia J, Mennan C, McCarthy HS, Roberts S, Richardson JB, Wright KT (2016)
600 Chondrogenic Potency Analyses of Donor-Matched Chondrocytes and Mesenchymal Stem
601 Cells Derived from Bone Marrow, Infrapatellar Fat Pad, and Subcutaneous Fat. *Stem Cells Int*
602 **2016**: 6969726.

603 Ghannam S, Bouffi C, Djouad F, Jorgensen C, Noel D (2010) Immunosuppression by
604 mesenchymal stem cells: mechanisms and clinical applications. *Stem Cell Res Ther* **1**: 2.

605 Gnecci M, Danieli P, Malpasso G, Ciuffreda MC (2016) Paracrine Mechanisms of
606 Mesenchymal Stem Cells in Tissue Repair. *Methods Mol Biol* **1416**: 123-146.

607 Gomez-Aristizabal A, Sharma A, Bakooshli MA, Kapoor M, Gilbert PM, Viswanathan
608 S, Gandhi R (2017) Stage-specific differences in secretory profile of mesenchymal stromal cells
609 (MSCs) subjected to early- vs late-stage OA synovial fluid. *Osteoarthritis Cartilage* **25**: 737-
610 741.

611 Grande DA, Pitman MI, Peterson L, Menche D, Klein M (1989) The repair of
612 experimentally produced defects in rabbit articular cartilage by autologous chondrocyte
613 transplantation. *J Orthop Res* **7**: 208-218.

614 Guimaraes-Camboa N, Cattaneo P, Sun Y, Moore-Morris T, Gu Y, Dalton ND,
615 Rockenstein E, Masliah E, Peterson KL, Stallcup WB, Chen J, Evans SM (2017) Pericytes of
616 Multiple Organs Do Not Behave as Mesenchymal Stem Cells In Vivo. *Cell Stem Cell* **20**: 345-
617 359 e345.

618 Heo JS, Choi Y, Kim HS, Kim HO (2016) Comparison of molecular profiles of human
619 mesenchymal stem cells derived from bone marrow, umbilical cord blood, placenta and adipose
620 tissue. *Int J Mol Med* **37**: 115-125.

621 Hsiao ST, Asgari A, Lokmic Z, Sinclair R, Dusting GJ, Lim SY, Dilley RJ (2012)
622 Comparative analysis of paracrine factor expression in human adult mesenchymal stem cells
623 derived from bone marrow, adipose, and dermal tissue. *Stem Cells Dev* **21**: 2189-2203.

624 Islam A, Hansen AK, Mennan C, Martinez-Zubiaurre I (2016) Mesenchymal stromal
625 cells from human umbilical cords display poor chondrogenic potential in scaffold-free three
626 dimensional cultures. *Eur Cell Mater* **31**: 407-424.

627 Islam A, Romijn EI, Lilledahl MB, Martinez-Zubiaurre I (2017) Non-linear optical
628 microscopy as a novel quantitative and label-free imaging modality to improve the assessment
629 of tissue-engineered cartilage. *Osteoarthritis Cartilage* **25**: 1729-1737.

630 Iso Y, Spees JL, Serrano C, Bakondi B, Pochampally R, Song YH, Sobel BE,
631 Delafontaine P, Prockop DJ (2007) Multipotent human stromal cells improve cardiac function

632 after myocardial infarction in mice without long-term engraftment. *Biochem Biophys Res*
633 *Commun* **354**: 700-706.

634 Jaguin M, Houlbert N, Fardel O, Lecureur V (2013) Polarization profiles of human M-
635 CSF-generated macrophages and comparison of M1-markers in classically activated
636 macrophages from GM-CSF and M-CSF origin. *Cell Immunol* **281**: 51-61.

637 Jin HJ, Bae YK, Kim M, Kwon SJ, Jeon HB, Choi SJ, Kim SW, Yang YS, Oh W, Chang
638 JW (2013) Comparative analysis of human mesenchymal stem cells from bone marrow, adipose
639 tissue, and umbilical cord blood as sources of cell therapy. *Int J Mol Sci* **14**: 17986-18001.

640 Karaoz E, Cetinalp Demircan P, Erman G, Gungorurler E, Eker Sariboyaci A (2017)
641 Comparative Analyses of Immunosuppressive Characteristics of Bone-Marrow, Wharton's
642 Jelly, and Adipose Tissue-Derived Human Mesenchymal Stem Cells. *Turk J Haematol* **34**: 213-
643 225.

644 Kondo M, Yamaoka K, Sonomoto K, Fukuyo S, Oshita K, Okada Y, Tanaka Y (2013)
645 IL-17 inhibits chondrogenic differentiation of human mesenchymal stem cells. *PLoS One* **8**:
646 e79463.

647 Lee WY-w, Wang B (2017) Cartilage repair by mesenchymal stem cells: Clinical trial
648 update and perspectives. *Journal of Orthopaedic Translation* **9**: 76-88.

649 Li CY, Wu XY, Tong JB, Yang XX, Zhao JL, Zheng QF, Zhao GB, Ma ZJ (2015)
650 Comparative analysis of human mesenchymal stem cells from bone marrow and adipose tissue
651 under xeno-free conditions for cell therapy. *Stem Cell Res Ther* **6**: 55.

652 Liechty KW, MacKenzie TC, Shaaban AF, Radu A, Moseley AM, Deans R, Marshak
653 DR, Flake AW (2000) Human mesenchymal stem cells engraft and demonstrate site-specific
654 differentiation after in utero transplantation in sheep. *Nat Med* **6**: 1282-1286.

655 Lohan P, Treacy O, Lynch K, Barry F, Murphy M, Griffin MD, Ritter T, Ryan AE
656 (2016) Culture expanded primary chondrocytes have potent immunomodulatory properties and
657 do not induce an allogeneic immune response. *Osteoarthritis Cartilage* **24**: 521-533.

658 Manferdini C, Paoletta F, Gabusi E, Gambari L, Piacentini A, Filardo G, Fleury-
659 Cappellesso S, Barbero A, Murphy M, Lisignoli G (2017) Adipose stromal cells mediated
660 switching of the pro-inflammatory profile of M1-like macrophages is facilitated by PGE₂: in
661 vitro evaluation. *Osteoarthritis Cartilage* **25**: 1161-1171.

662 Miwa M, Saura R, Hirata S, Hayashi Y, Mizuno K, Itoh H (2000) Induction of apoptosis
663 in bovine articular chondrocyte by prostaglandin E₂ through cAMP-dependent pathway.
664 *Osteoarthritis Cartilage* **8**: 17-24.

665 Muthuri SG, McWilliams DF, Doherty M, Zhang W (2011) History of knee injuries and
666 knee osteoarthritis: a meta-analysis of observational studies. *Osteoarthritis Cartilage* **19**: 1286-
667 1293.

668 Najar M, Raicevic G, Kazan HF, De Bruyn C, Bron D, Toungouz M, Lagneaux L (2012)
669 Immune-Related Antigens, Surface Molecules and Regulatory Factors in Human-Derived
670 Mesenchymal Stromal Cells: The Expression and Impact of Inflammatory Priming. *Stem Cell*
671 *Reviews and Reports* **8**: 1188-1198.

672 Ogura T, Bryant T, Minas T (2017) Long-term Outcomes of Autologous Chondrocyte
673 Implantation in Adolescent Patients. *The American Journal of Sports Medicine* **45**: 1066-1074.

674 Otsuka S, Aoyama T, Furu M, Ito K, Jin Y, Nasu A, Fukiage K, Kohno Y, Maruyama
675 T, Kanaji T, Nishiura A, Sugihara H, Fujimura S, Otsuka T, Nakamura T, Toguchida J (2009)
676 PGE₂ signal via EP₂ receptors evoked by a selective agonist enhances regeneration of injured
677 articular cartilage. *Osteoarthritis Cartilage* **17**: 529-538.

678 Ozeki N, Muneta T, Koga H, Nakagawa Y, Mizuno M, Tsuji K, Mabuchi Y, Akazawa
679 C, Kobayashi E, Matsumoto K, Futamura K, Saito T, Sekiya I (2016) Not single but periodic

680 injections of synovial mesenchymal stem cells maintain viable cells in knees and inhibit
681 osteoarthritis progression in rats. *Osteoarthritis Cartilage* **24**: 1061-1070.

682 Papadopoulou A, Yiangou M, Athanasiou E, Zogas N, Kaloyannidis P, Batsis I, Fassas
683 A, Anagnostopoulos A, Yannaki E (2012) Mesenchymal stem cells are conditionally
684 therapeutic in preclinical models of rheumatoid arthritis. *Ann Rheum Dis* **71**: 1733-1740.

685 Peeters CM, Leijns MJ, Reijman M, van Osch GJ, Bos PK (2013) Safety of intra-articular
686 cell-therapy with culture-expanded stem cells in humans: a systematic literature review.
687 *Osteoarthritis Cartilage* **21**: 1465-1473.

688 Poree B, Kyriotou M, Chadjichristos C, Beauchef G, Renard E, Legendre F, Melin M,
689 Gueret S, Hartmann DJ, Mallein-Gerin F, Pujol JP, Boumediene K, Galera P (2008) Interleukin-
690 6 (IL-6) and/or soluble IL-6 receptor down-regulation of human type II collagen gene
691 expression in articular chondrocytes requires a decrease of Sp1.Sp3 ratio and of the binding
692 activity of both factors to the COL2A1 promoter. *J Biol Chem* **283**: 4850-4865.

693 Prockop DJ (2009) Repair of tissues by adult stem/progenitor cells (MSCs):
694 controversies, myths, and changing paradigms. *Mol Ther* **17**: 939-946.

695 Rehman J, Traktuev D, Li J, Merfeld-Clauss S, Temm-Grove CJ, Bovenkerk JE, Pell
696 CL, Johnstone BH, Considine RV, March KL (2004) Secretion of angiogenic and antiapoptotic
697 factors by human adipose stromal cells. *Circulation* **109**: 1292-1298.

698 Sato K, Kondo M, Sakuta K, Hosoi A, Noji S, Sugiura M, Yoshida Y, Kakimi K (2009)
699 Impact of culture medium on the expansion of T cells for immunotherapy. *Cytotherapy* **11**: 936-
700 946.

701 Saulnier N, Viguier E, Perrier-Groult E, Chenu C, Pillet E, Roger T, Maddens S,
702 Boulocher C (2015) Intra-articular administration of xenogeneic neonatal Mesenchymal
703 Stromal Cells early after meniscal injury down-regulates metalloproteinase gene expression in

704 synovium and prevents cartilage degradation in a rabbit model of osteoarthritis. *Osteoarthritis*
705 *Cartilage* **23**: 122-133.

706 Singh A, Goel SC, Gupta KK, Kumar M, Arun GR, Patil H, Kumaraswamy V, Jha S
707 (2014) The role of stem cells in osteoarthritis: An experimental study in rabbits. *Bone Joint Res*
708 **3**: 32-37.

709 Snelling SJ, Bas S, Puskas GJ, Dakin SG, Suva D, Finckh A, Gabay C, Hoffmeyer P,
710 Carr AJ, Lubbeke A (2017) Presence of IL-17 in synovial fluid identifies a potential
711 inflammatory osteoarthritic phenotype. *PLoS One* **12**: e0175109.

712 Subramanian A, Fong CY, Biswas A, Bongso A (2015) Comparative Characterization
713 of Cells from the Various Compartments of the Human Umbilical Cord Shows that the
714 Wharton's Jelly Compartment Provides the Best Source of Clinically Utilizable Mesenchymal
715 Stem Cells. *PLoS One* **10**: e0127992.

716 Sui Y, Lee JH, DiMicco MA, Vanderploeg EJ, Blake SM, Hung HH, Plaas AH, James
717 IE, Song XY, Lark MW, Grodzinsky AJ (2009) Mechanical injury potentiates proteoglycan
718 catabolism induced by interleukin-6 with soluble interleukin-6 receptor and tumor necrosis
719 factor alpha in immature bovine and adult human articular cartilage. *Arthritis Rheum* **60**: 2985-
720 2996.

721 Tang X, Fan L, Pei M, Zeng L, Ge Z (2015) Evolving concepts of chondrogenic
722 differentiation: history, state-of-the-art and future perspectives. *Eur Cell Mater* **30**: 12-27.

723 Treacy O, O'Flynn L, Ryan AE, Morcos M, Lohan P, Schu S, Wilk M, Fahy G, Griffin
724 MD, Nosov M, Ritter T (2014) Mesenchymal stem cell therapy promotes corneal allograft
725 survival in rats by local and systemic immunomodulation. *Am J Transplant* **14**: 2023-2036.

726 van Buul GM, Villafuertes E, Bos PK, Waarsing JH, Kops N, Narcisi R, Weinans H,
727 Verhaar JA, Bernsen MR, van Osch GJ (2012) Mesenchymal stem cells secrete factors that

728 inhibit inflammatory processes in short-term osteoarthritic synovium and cartilage explant
729 culture. *Osteoarthritis Cartilage* **20**: 1186-1196.

730 Vogel DY, Glim JE, Stavenuiter AW, Breur M, Heijnen P, Amor S, Dijkstra CD, Beelen
731 RH (2014) Human macrophage polarization in vitro: maturation and activation methods
732 compared. *Immunobiology* **219**: 695-703.

733 von Bahr L, Sundberg B, Lonnie L, Sander B, Karbach H, Hagglund H, Ljungman P,
734 Gustafsson B, Karlsson H, Le Blanc K, Ringden O (2012) Long-term complications,
735 immunologic effects, and role of passage for outcome in mesenchymal stromal cell therapy.
736 *Biol Blood Marrow Transplant* **18**: 557-564.

737 Vonk LA, de Windt TS, Slaper-Cortenbach IC, Saris DB (2015) Autologous, allogeneic,
738 induced pluripotent stem cell or a combination stem cell therapy? Where are we headed in
739 cartilage repair and why: a concise review. *Stem Cell Res Ther* **6**: 94.

740 Wang Z, Zheng C, Zhong Y, He J, Cao X, Xia H, Ba H, Li P, Wu S, Peng C (2017)
741 Interleukin-17 Can Induce Osteoarthritis in Rabbit Knee Joints Similar to Hulth's Method.
742 *Biomed Res Int* **2017**: 2091325.

743 Wei J, Sun Z, Chen Q, Gu J (2006) Serum deprivation induced apoptosis in macrophage
744 is mediated by autocrine secretion of type I IFNs. *Apoptosis* **11**: 545-554.

745 Wolfstadt JI, Cole BJ, Ogilvie-Harris DJ, Viswanathan S, Chahal J (2015) Current
746 concepts: the role of mesenchymal stem cells in the management of knee osteoarthritis. *Sports*
747 *Health* **7**: 38-44.

748 Xu YK, Ke Y, Wang B, Lin JH (2015) The role of MCP-1-CCR2 ligand-receptor axis
749 in chondrocyte degradation and disease progress in knee osteoarthritis. *Biol Res* **48**: 64.

750 Yang X, Zhu TY, Wen LC, Cao YP, Liu C, Cui YP, Meng ZC, Liu H (2015)
751 Intraarticular Injection of Allogenic Mesenchymal Stem Cells has a Protective Role for the
752 Osteoarthritis. *Chin Med J (Engl)* **128**: 2516-2523.

753 Zhang P, Zhong ZH, Yu HT, Liu B (2015) Exogenous expression of IL-1Ra and TGF-
754 beta1 promotes in vivo repair in experimental rabbit osteoarthritis. *Scand J Rheumatol* **44**: 404-
755 411.

756 Zhao XY, Yang ZB, Zhang ZJ, Zhang ZQ, Kang Y, Huang GX, Wang SW, Huang H,
757 Liao WM (2015) CCL3 serves as a potential plasma biomarker in knee degeneration
758 (osteoarthritis). *Osteoarthritis Cartilage* **23**: 1405-1411.

759 **Figure legends**

760 **Figure 1. Hierarchical clustering of identified proteins from secretomes of ACs, HFPSCs,**
761 **SMSCs and UCSCs. A.** Venn diagram depicts the percentage of identified proteins shared
762 among four different stromal cell types. **B.** Dendrogram shows two major clusters of four
763 different stromal cell types. All cell sources from adult mesenchyme origin clustered together,
764 whereas the four donors of UCSCs from extra-embryonic origin clustered separately.

765 **Figure 2. Protein expression analysis by LC-MS/MS from conditioned medium of ACs,**
766 **HFPSCs, SMSCs and UCSCs. A.** Distribution of identified proteins into six main categories
767 according to their function annotated using GOBP terms. **B.** Volcano plot illustrates the results
768 of the six sets of statistical comparisons made between HFPSCs vs ACs, SMSCs vs ACs,
769 HFPSCs vs SMSCs, UCSCs vs ACs, UCSCs vs HFPSCs and UCSCs vs SMSCs. These plots
770 show each protein with $-\text{Log}_{10}(p\text{-value})$ and Log_{10} of fold change of the comparison on the
771 Y-axis and X-axis, respectively. Proteins with greater fold change and lower p -value are plotted
772 further away from zero on each axis. Proteins that are significantly up and down-regulated ($p <$
773 0.01) are presented in green and red colour, respectively.

774 **Figure 3. Comparative expression of selected proteins from conditioned medium of ACs,**
775 **HFPSCs, SMSCs and UCSCs.** The heat map shows proteins involved in **A.** ECM remodelling
776 (proteases and inhibitors), **B.** cell signalling (growth factors) and **C.** inflammation/immune

777 responses. Down-regulated proteins are indicated in red, whereas up-regulated proteins are in
778 blue.

779 **Figure 4. Comparison of identified cytokines and chemokines from conditioned medium**
780 **of ACs, HFPSCs, SMSCs and UCSCs.** Dot density show concentration of cytokines involved
781 in inflammation (IL-4, IL-6, IL-8, IL-12, IL-17 and PGE2) and chemokines (MCP-1, MIP-1 α
782 and RANTES) detected in supernatants of four different stromal cell types. Level of
783 significance is p (*) < 0.05.

784 **Figure 5. Comparison of identified MMPs and anabolic factors from conditioned medium**
785 **of ACs, HFPSCs, SMSCs and UCSCs.** Dot density shows the concentration of MMPs (MMP-
786 1, MMP-3, MMP-7 and MMP-9) and growth factors (TGF- β 1, bFGF and BMP-2) detected in
787 supernatants of four different stromal cell types. Level of significance is p (*) < 0.05.

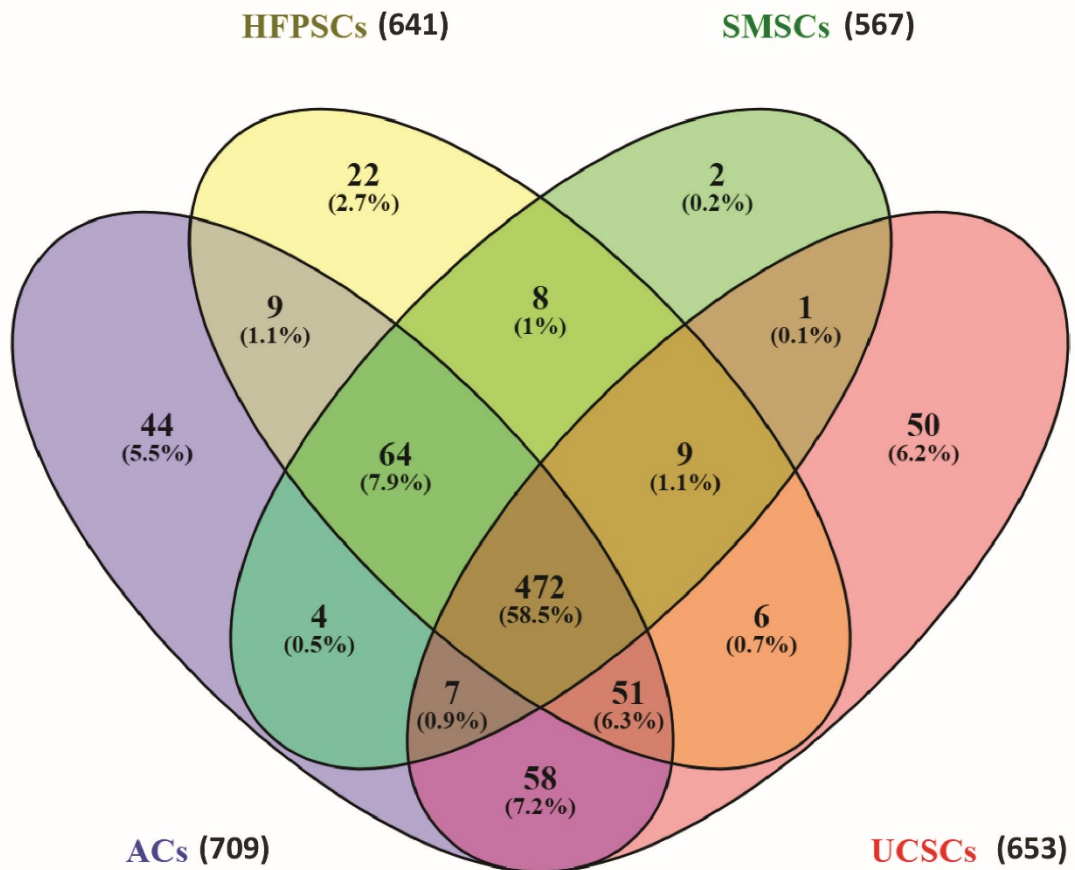
788 **Figure 6. Differential modulation of PBMCs activation by MSCs conditioned medium. A.**
789 PBMCs proliferation assay: representative flow cytometry dot plots depict the percentage of
790 CFSE labelled PBMCs stimulated with 10 μ g/mL of PHA in presence and absence of CM from
791 the four different stromal cell types. **B.** Quantitative analyses of PBMCs proliferation and
792 migration in presence and absence of CM from four different stromal cell types. SDF-1 at 100
793 ng/mL was used for chemo-attraction in migration assays **C.** Total concentration of TNF- α , and
794 IFN- γ detected in PBMCs-CM (10⁶ cells/well) after incubation with PHA and CM from four
795 different stromal cell types. Level of significance is p (*) < 0.05.

796 **Figure 7. UCSCs secretomes can modulate macrophage-mediated inflammation. A.**
797 Characterisation of surface molecules during polarisation of M0-M into M1-M (CD40, CD64,
798 CD80, CD86 and HLA-DR) and M2-M (CD163) by flow cytometry. Red, blue and orange peak
799 represents isotype control, M0-M and activated macrophages, respectively. **B.** Dot density
800 depicts M1-M activation and distinct blocking of M1-M activation by CM from ACs, HFPSCs,

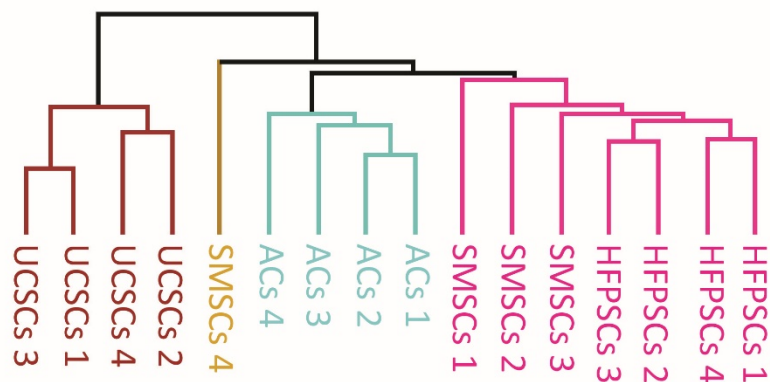
801 SMSCs and UCSCs. M2-M polarisation was used as a negative control for surface expression
802 of CD40 and HLA-DR. C. Levels of TNF- α , IL-6 and IL-12 detected in macrophage culture
803 conditioned medium (2.5×10^6 cells/well) after incubation with CM from four different stromal
804 cell types. Level of significances are $p < 0.05$ (*) and $p < 0.005$ (**).

805 **Figure 8. Comparison between serum-free and serum-containing conditioned medium of**
806 **ACs, HFSPCs, SMSCs and UCSCs.** Presence of serum increases the production of IL-6 by
807 all cell types.

A.



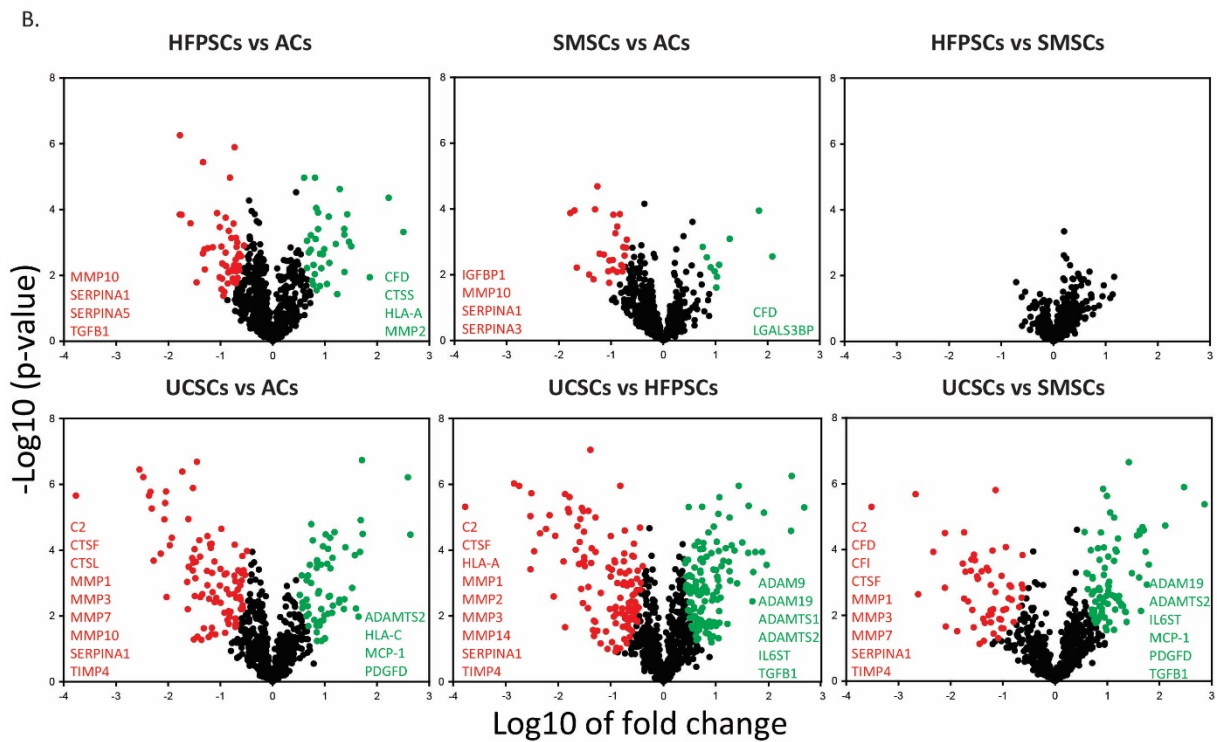
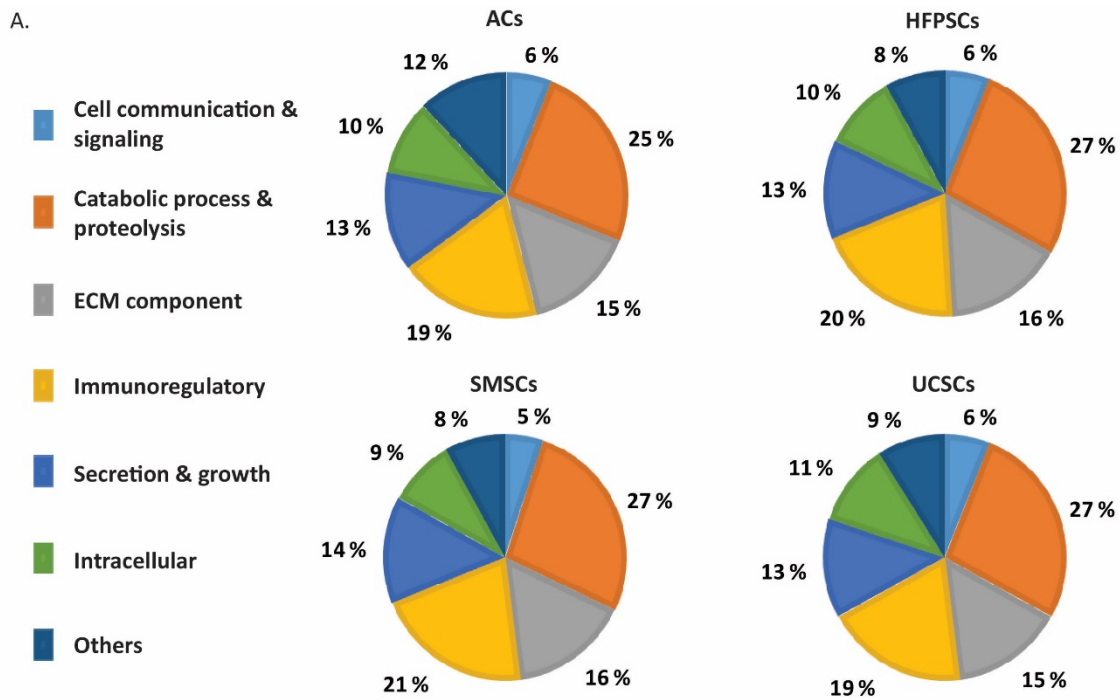
B.



808

809 Figure 1: Hierarchical clustering of identified proteins from secretomes of ACs, HFPSCs,
 810 SMSCs and UCSCs.

811

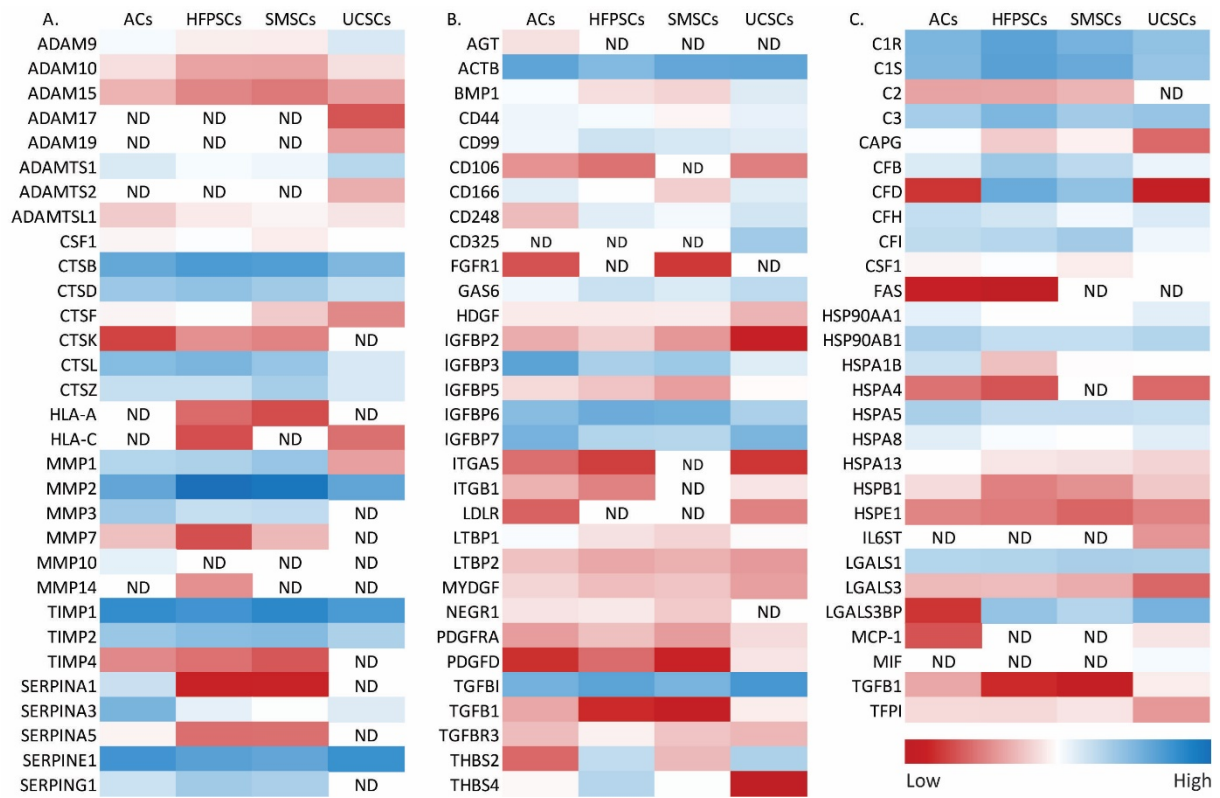


812

813 Figure 2. Protein expression analysis by LC-MS/MS from conditioned medium of ACs,
 814 HFPSCs, SMSCs and UCSCs.

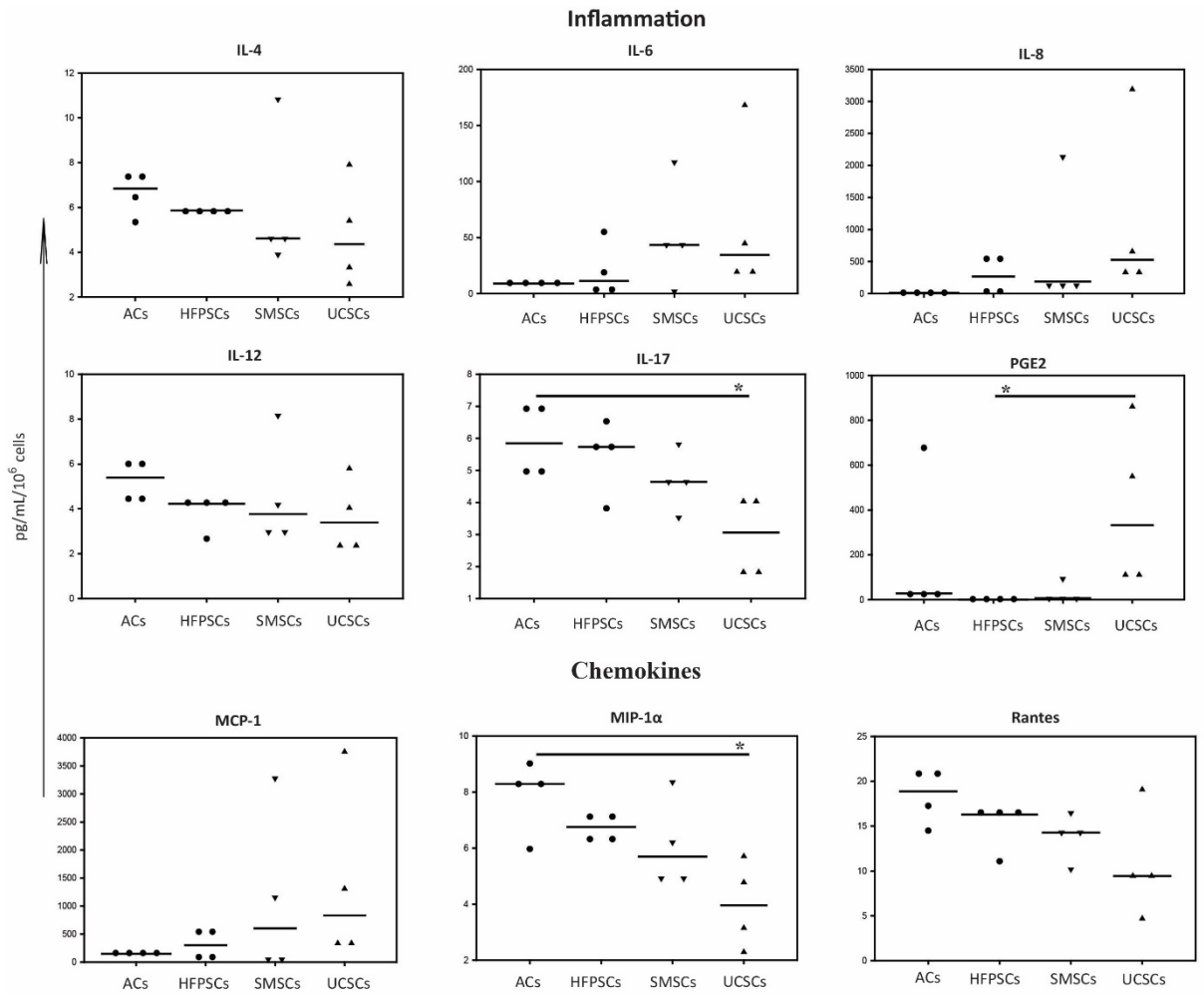
815

816



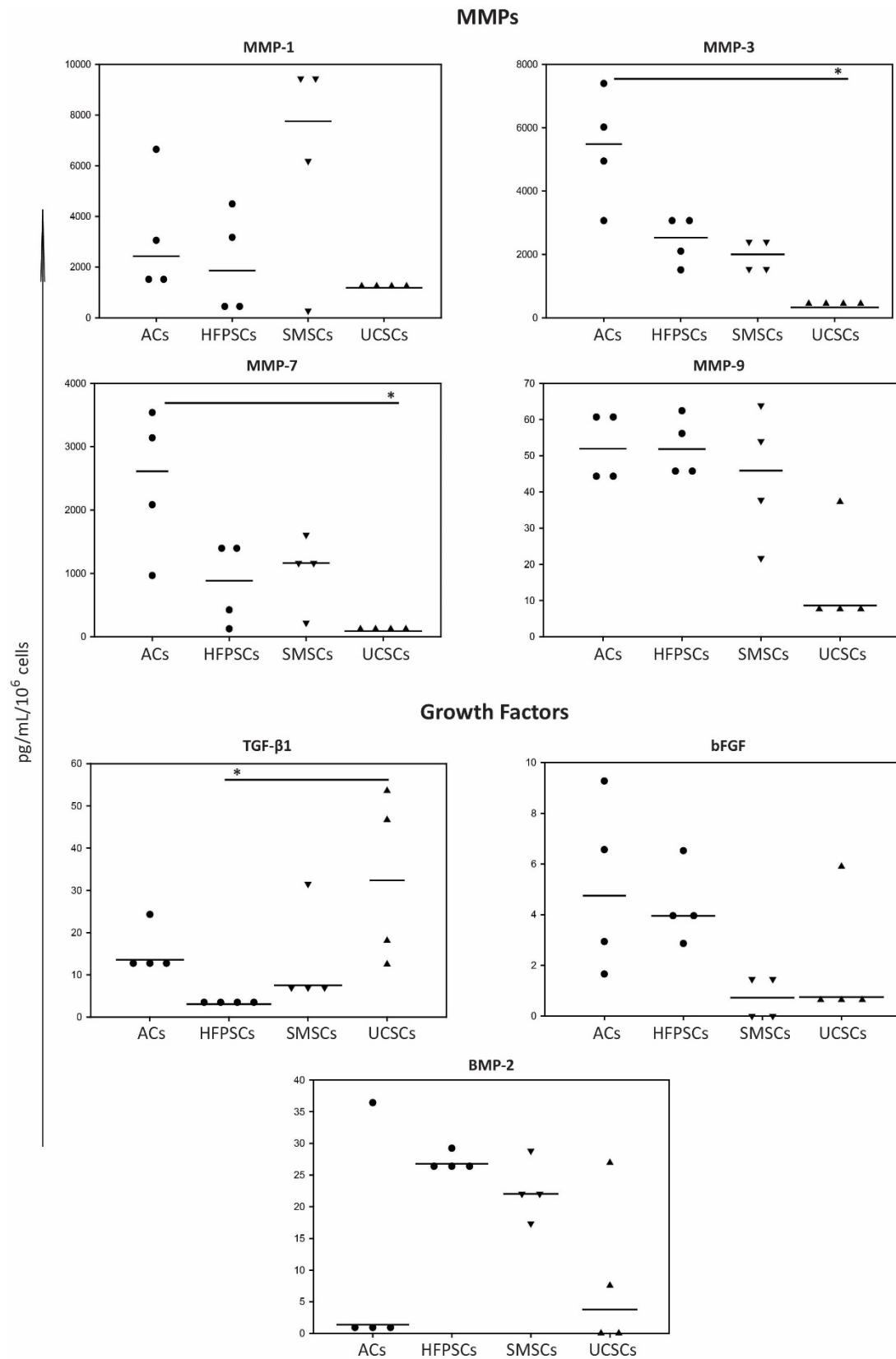
817

818 Figure 3. Comparative expression of selected proteins from conditioned medium of ACs,
 819 HFPCs, SMSCs and UCSCs.



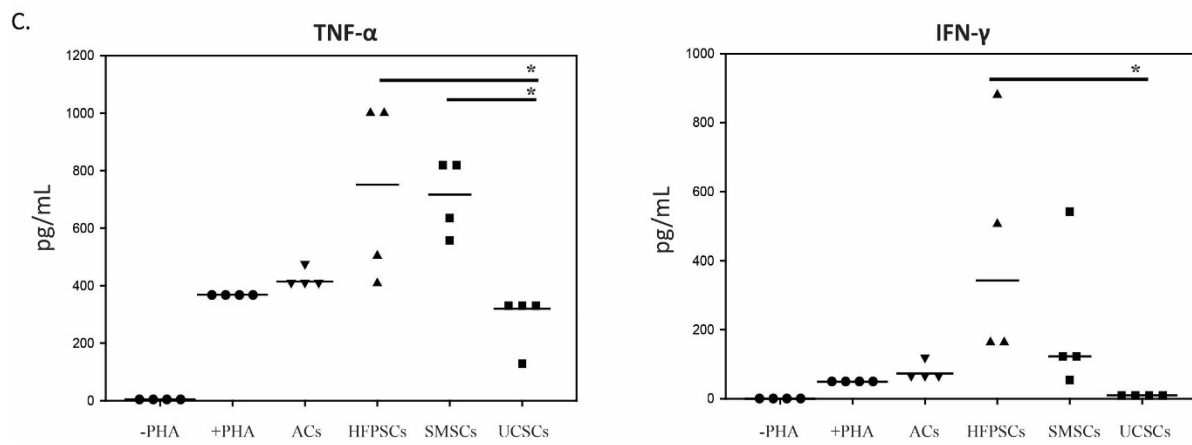
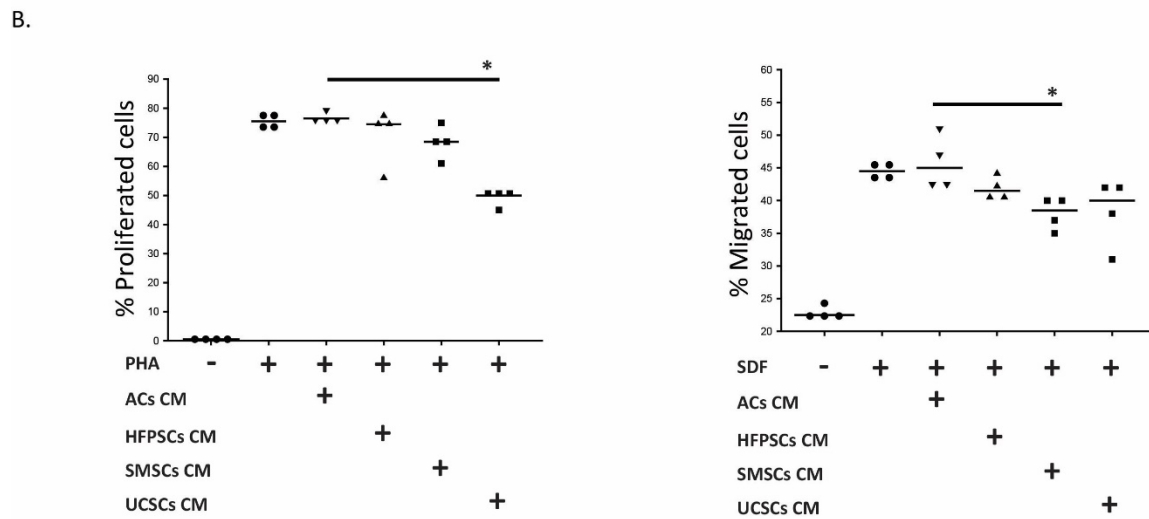
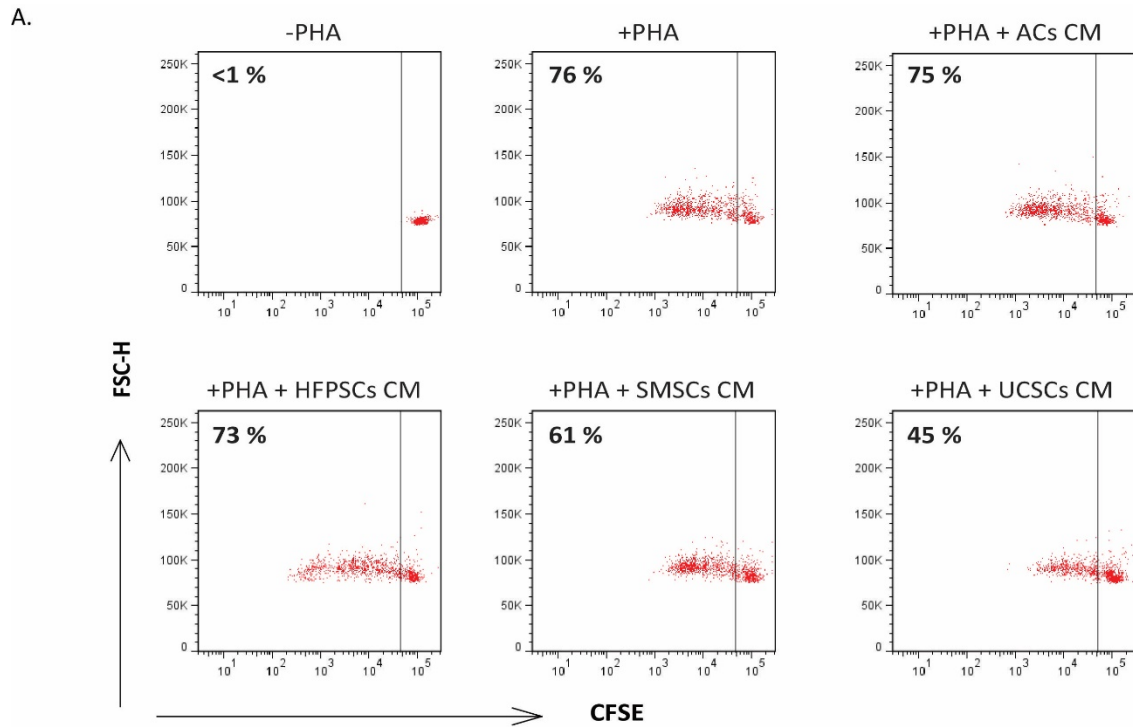
820

821 Figure 4. Comparison of identified cytokines and chemokines from conditioned medium of
 822 ACs, HFPCs, SMSCs and UCSCs.



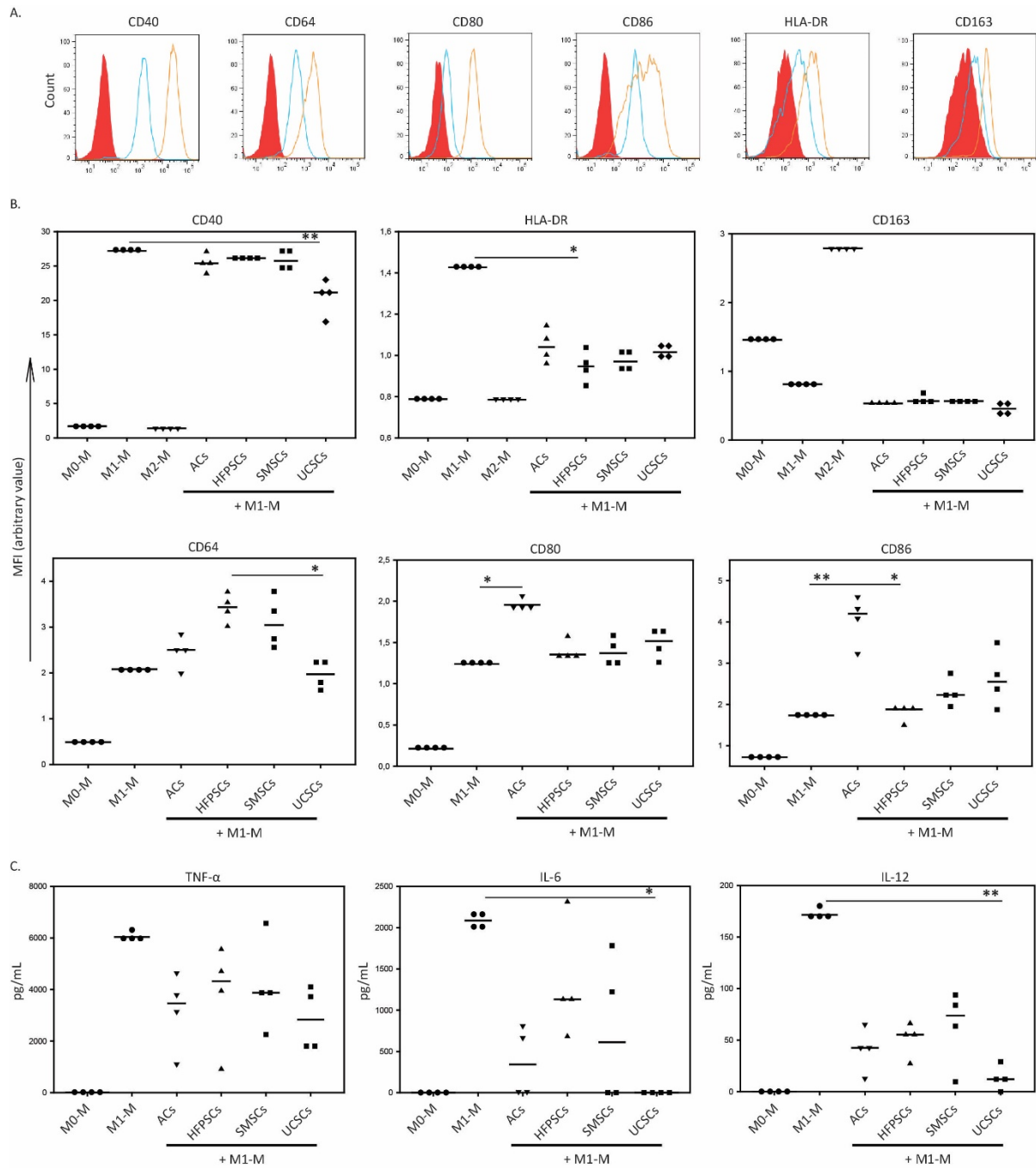
823

824 Figure 5. Comparison of identified MMPs and anabolic factors from conditioned medium of
 825 ACs, HFPCs, SMSCs and UCSCs.



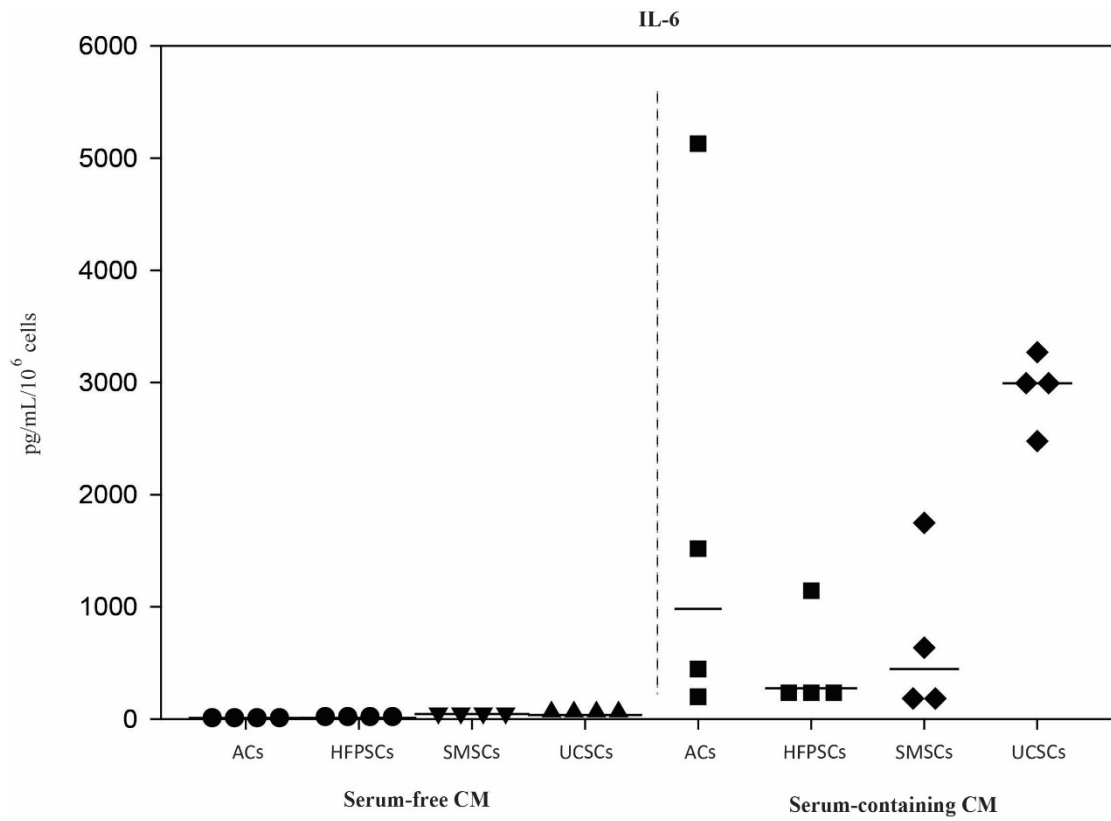
826

827 Figure 6. Differential modulation of PBMCs activation by MSCs conditioned medium.



828

829 Figure 7. UCSCs secretomes can modulate macrophage-mediated inflammation.



830

831 Figure 8. Comparison between serum-free and serum-containing conditioned medium of ACs,
 832 HFPSCs, SMSCs and UCSCs.